J Appl Physiol 137: 616–628, 2024.
First published July 18, 2024; doi:10.1152/japplphysiol.00253.2024

american physiological society

JOURNAL OF APPLIED PHYSIOLOGY

RESEARCH ARTICLE

Biomechanics of human locomotion in the wind

Raphael M. Mesquita,[1] Patrick A. Willems,[1] Giovanna Catavitello,[1] Giuseppe Gibertini,[2] Valentina Natalucci,[3] Francesco Luciano,[3] Alberto Enrico Minetti,[3] Gaspare Pavei,[3] and Arthur H. Dewolf[1]

[1]*Laboratory of Physiology and Biomechanics of Locomotion, Institute of NeuroScience, Université catholique de Louvain, Louvain-la-Neuve, Belgium;* [2]*Department of Aerospace Science and Technology, Politecnico di Milano, Milan, Italy; and* [3]*Laboratory of Physiomechanics, Department of Pathophysiology and Transplantation–Division of Physiology, University of Milan, Milan, Italy*

Abstract

In laboratory settings, human locomotion encounters minimal opposition from air resistance. However, moving in nature often requires overcoming airflow. Here, the drag force exerted on the body by different headwind or tailwind speeds (between 0 and 15 m·s^{-1}) was measured during walking at 1.5 m·s^{-1} and running at 4 m·s^{-1}. To our knowledge, the biomechanical effect of drag in human locomotion has only been evaluated by simulations. Data were collected on eight male subjects using an instrumented treadmill placed in a wind tunnel. From the ground reaction forces, the drag and external work done to overcome wind resistance and to sustain the motion of the center of mass of the body were measured. Drag increased with wind speed: a 15 m·s^{-1} headwind exerted a drag of ∼60 N in walking and ∼50 N in running. The same tailwind exerted −55 N of drag in both gaits. At this wind speed, the work done to overcome the airflow represented ∼80% of the external work in walking and ∼50% in running. Furthermore, in the presence of fast wind speeds, subjects altered their drag area (C_dA) by adapting their posture to limit the increase in air friction. Moving in the wind modified the ratio between positive and negative external work performed. The modifications observed when moving with a head- or tailwind have been compared with moving uphill or downhill. The present findings may have implications for optimizing aerodynamic performance in competitive running, whether in sprints or marathons.

NEW & NOTEWORTHY This is the first study to assess the biomechanical adaptations to a wide range of wind speeds inside a wind tunnel. Humans increase their mechanical work and alter their drag area (C_dA) by adapting their posture when walking and running against increasing head and tailwinds. The observed drag force applied to the subject is different between walking and running at similar headwind speeds.

aerodynamics; external work; locomotion; wind tunnel

INTRODUCTION

Locomotion enables living beings to move from one point to another traversing a medium that typically offers resistance to their forward motion: bacteria travel through extracellular fluid, fish through water, birds through air, etc. (1). When moving on land, most animals use their limbs to support their weight, propel themselves forward and exert force to overcome inertia and counter air resistance. In this case, external work (W_{ext}) is done *1*) against air resistance and *2*) during interaction of the body with the ground (2). Additionally, because in legged locomotion the limbs must constantly be "reset: for the following step, internal work (W_{int}) is also required to move the limbs relative to the center of mass (CoM; see GLOSSARY for abbreviations) (3).

Air resistance, or drag, is an external force against which the muscle-tendon units (MTUs) do work. Its magnitude is directly related to the drag area (C_dA), i.e., the projected frontal area facing the airflow (A) multiplied by the drag coefficient (C_d) and by the dynamic pressure generated by the air moving around the body at a certain speed (4). In turn, the product of the drag and the distance covered represents W_{drag}, the work required to overcome the resistance of the medium. Secondly, the interaction of the body with the ground is responsible for the remaining portion of external work. If the feet are not skidding, no work is done against frictional forces on the ground. Therefore, the ground reaction force (GRF) is responsible for the kinetic and potential energy changes of the CoM during each step (2). Consequently, the MTUs mainly perform work to sustain the movements of the CoM relative to the surroundings (W_{com}) (2).

When moving in still air, the speed of the relative airflow generated is equal to the subject's moving speed. In human locomotion, this speed is generally low i.e., less than 25 km·h^{-1}, equating to negligible drag: e.g., at 21 km·h^{-1}, the

Correspondence: A. Dewolf (arthur.dewolf@uclouvain.be).
Submitted 5 April 2024 / Revised 15 July 2024 / Accepted 16 July 2024

magnitude of air resistance represents ~6 N (5–9). As a result, the work done to sustain the movements of the CoM against drag (W_{drag}) represents only a small fraction of the total positive work ($W_{tot} = W_{ext} + W_{int}$) done during locomotion: <3% in walking and <10% in running (10). Consequently, as a first approximation, W_{drag} is negligible in still air, except at high running speeds (8, 11). However, in the presence of a faster head- or tailwind, the additional external force generated by the airflow will hinder/aid the progression of the person and will most likely also alter the walking and running gait mechanics.

The first goal of our study was to quantify the drag exerted on the subject at different wind speeds (ranging from −15 to +15 $m \cdot s^{-1}$) while walking at 1.5 $m \cdot s^{-1}$ and running at 4 $m \cdot s^{-1}$. To our knowledge, air resistance in human locomotion has only been evaluated using simulations such as computational fluid dynamics (CFD) models or manikins that simulate the human body (9, 12–16) or investigated via experimental studies, e.g., by using external tractive devices to pull on the subject and thus hindering or aiding progression (17–20). Regarding human locomotion, CFD simulations have, among others, studied the drag applied on the body and their respective segments (9, 12) and the effect of multiple runner formations on running performance (13, 14, 16, 18, 21, 22). However, little full-scale experimental data have been collected in a wind tunnel (5, 7, 8). Moreover, to the best of our knowledge, there have been no studies investigating the biomechanical adjustments of locomotion when moving against the wind.

Here, in a novel approach, the aerodynamic drag of humans walking and running on a treadmill in a wind tunnel was measured via the ground reaction forces (6). This investigation is of current relevance (13, 14, 16), especially in the field of sports science where the official marathon world record is on the brink of passing below the 2-h mark (23). We anticipated that as an adaption to the increased resistive force, subjects would adjust their posture, and consequently their C_dA, to reduce air resistance. This phenomenon is commonly observed in various organisms experiencing flow influences (24).

The second goal of the present study was to analyze the effect of drag on the pendular mechanism of walking and the bouncing mechanism of running. When moving in still air, since $W_{drag} \approx 0$, one can state that the positive (W^+_{ext}) and negative (W^-_{ext}) work done are about equal (25). When wind speed increases, the W_{ext} should increase. In the case of headwind, W_{drag} is positive and slows the CoM. Consequently, $W^+_{ext} > W^-_{ext}$, meaning that MTUs do more positive than negative work to maintain a constant average speed of progression. In the opposite situation (i.e., tailwind), the flowing air does work on the subject and $W^-_{ext} > W^+_{ext}$, meaning that MTUs do more negative than positive work. This hypothesis is based on what occurs when moving against a hindering/aiding tractive force pulling on the CoM (17, 26). One may expect that the deviation from a 1.0 ratio between positive and negative work will affect the pendulum-like mechanism of walking and bouncing mechanism of running (25). Indeed, these models are characterized by a phase lag between the kinetic energy of the CoM due to its fore-aft motion (E_{kf}) and the energy due to its vertical motion (E_v) (2). When moving in still air on a flat terrain, the time course of E_{kf} and E_v are out of phase during walking and in phase during running. In the presence of linear head- or tailwind, E_v will most likely not change, as the external force is applied in the fore-aft direction. On the contrary, the amplitude of positive work to accelerate the CoM will be greater/smaller than the negative work to decelerate the CoM. This situation may be similar to walking/running on a slope (27–30), when the ratio between negative and positive work changes, their respective durations are also modified, inducing a change in the phase shift between E_v and E_{kf}. Therefore we hypothesized that, as in walking/running against an external tractive force or on a slope (17, 18, 26, 29, 30), the phase relationship will change and modify the energy transduction between kinetic and potential energy (31).

To achieve these goals, we evaluated eight subjects walking at 1.5 $m \cdot s^{-1}$ and running at 4 $m \cdot s^{-1}$ on an instrumented treadmill in a wind tunnel against different head- and tailwind blowing at different speeds. The GRF was recorded, and the mechanics of the CoM applied against head- and tailwind forces were analyzed.

METHODS

Experimental Setup

The experimental setup described here was also used in the context of a recently published study (6). An instrumented treadmill (Stellar, h/p/Cosmos, Nussdorf, Germany; Arsalis, Genappe, Belgium) with a belt surface of 1.6 × 0.65 m was fixed in the center of a 4 m wide × 6 m long ×3.84 m high wind tunnel at the GVPM, Politecnico di Milano (Italy). The wind tunnel free stream turbulent level was less than 0.1%. The treadmill was aligned so that its long axis was parallel to the direction of the wind. To ensure a smooth (more laminar) flow around the athlete, a wooden floor structure was built around the treadmill and was oriented so that the wind first touched the subject before reaching the treadmill motor. In this way, the motor wake did not affect the test (Fig. 1 and Supplemental Fig. S1). The flow disturbances introduced by the test rig were checked before athlete testing. In summary, the unavoidable turbulent boundary layer over the floor affected a region of less than 20 cm over the ground, and these differences in the local dynamic pressures (in respect to the reference value taken at 1 m over the floor) were sufficiently small to allow for an estimation of a maximum error of 3% on the body total drag due to the wind nonuniformity.

Four strain-gauge force transducers placed under the body of the treadmill measured the three components of the GRF. The force transducers were shielded by a thin aluminum plate to prevent wind from directly applying a force to the sensors. Before the data collection, the strain gauges were calibrated and the cross talk between vertical F_z and fore-aft F_f components of the GRF components were evaluated and remained on average below 0.5% (32). Furthermore, before each recording, the force offset was removed from the signal. The transducer's analog signals were amplified, low-pass filtered (4-pole Bessel filter with a −3-dB cut-off frequency at 200 Hz) to avoid an aliasing effect during digitization, and recorded with a sampling rate of 1 kHz (33). After digitization, the GRF signals were filtered by a two-way eighth-order Bessel filter with

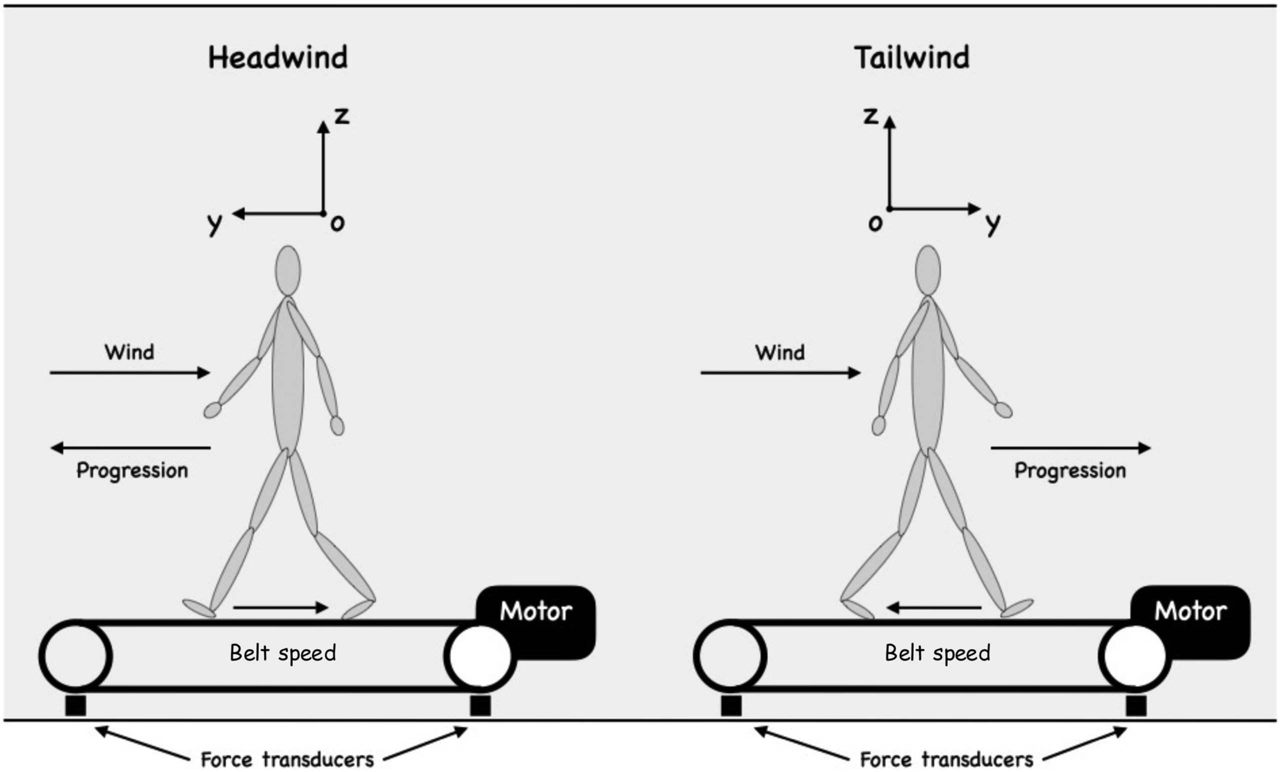

Figure 1. Illustration of the direction of the speed belt and of the forces applied to the subject when moving either with a head- or tailwind. In either wind direction, the wind first touched the subject before touching the motor, as such the motor wake did not affect the test conditions.

a lowpass cut-off frequency at 10 Hz for the lateral F_x, 20 Hz for F_y, and 30 Hz for F_z (34). A typical trace of the vertical and fore-aft components of the GRF is shown during walking (Fig. 2A) and during running (Fig. 3A).

The electrical motor of the belt was also instrumented with an optical angle encoder (Nussdorf, Germany; Arsalis, Genappe, Belgium) to measure the instantaneous velocity of the belt (v_{belt}). When the participants walked or ran on the treadmill, the recorded average velocity of the belt over a stride (V_{avg}) differed by 2.8 ± 1.4% from the chosen speed and the instantaneous v_{belt} did not change by more than 6% of V_{avg}.

Bilateral, full-body three-dimensional kinematics were recorded at 250 Hz by means of a VICON system (Oxford, UK) with eight cameras (6 MX-13 and 2 T20-S) placed around the treadmill. Participants were equipped with 18 retroreflective markers glued onto the skin. In the context of this study, only the markers glued on the zygomatic arch, shoulder, and greater trochanter were used to measure the angle between the long axis of the trunk and the horizontal. Kinematic data were then oversampled at 1 kHz using a linear interpolation function in LABVIEW. The kinematic data were filtered by the same lowpass filter as the ground reaction forces (cut-off frequency at 30 Hz). An oversampling of the kinematic data was chosen rather than a downsampling of the kinetic data to ensure that the force signal characteristics were not lost during data processing. Subjects also wore a face mask together with a portable gas analyzer on their back (K5, COSMED, Rome, Italy). The metabolic data will be a part of a forthcoming study.

Participants and Experimental Procedure

Eight professional or semiprofessional male runners (height: 1.77 ± 0.05 m, mass: 66 ± 7 kg, age: 31.2 ± 6.2 yr; Personal Best 10,000 m: 31 ft. 20 in. ± 1 ft. 12 in.; means ± SD) participated in the study. The number of subjects chosen was based on an a priori statistical power analysis using G*Power (35) from the results of a previous study that focused on similar variables (17). Informed written consent of each subject was obtained, and the study followed the guidelines of the Declaration of Helsinki. Subjects consented to having their photos published. All procedures were approved by the local ethics committee (Politecnico di Milano No. 16/2022).

Participants walked at 1.5 $m \cdot s^{-1}$ and ran at 4 $m \cdot s^{-1}$ on the instrumented treadmill, wearing a bathing suit and their usual, conventional running shoes (Figs. 2C and 3C). The subjects walked and ran in still air and against 10 different headwind (denominated as +) and tailwind (−) velocities of 0, ±5, ±7.5, ±10, ±12.5, and ±15 $m \cdot s^{-1}$.

The experimental protocol involved participants walking and running in both wind directions at a given wind speed before switching to the next randomly chosen wind speed.

Data Processing

Data processing was performed via custom-made programs written with LABVIEW (National Instruments 2019, Austin, TX). In both gait patterns, strides were defined as a succession of a right followed by a left step. A step started at foot contact, determined at the threshold when $F_z > 30$ N,

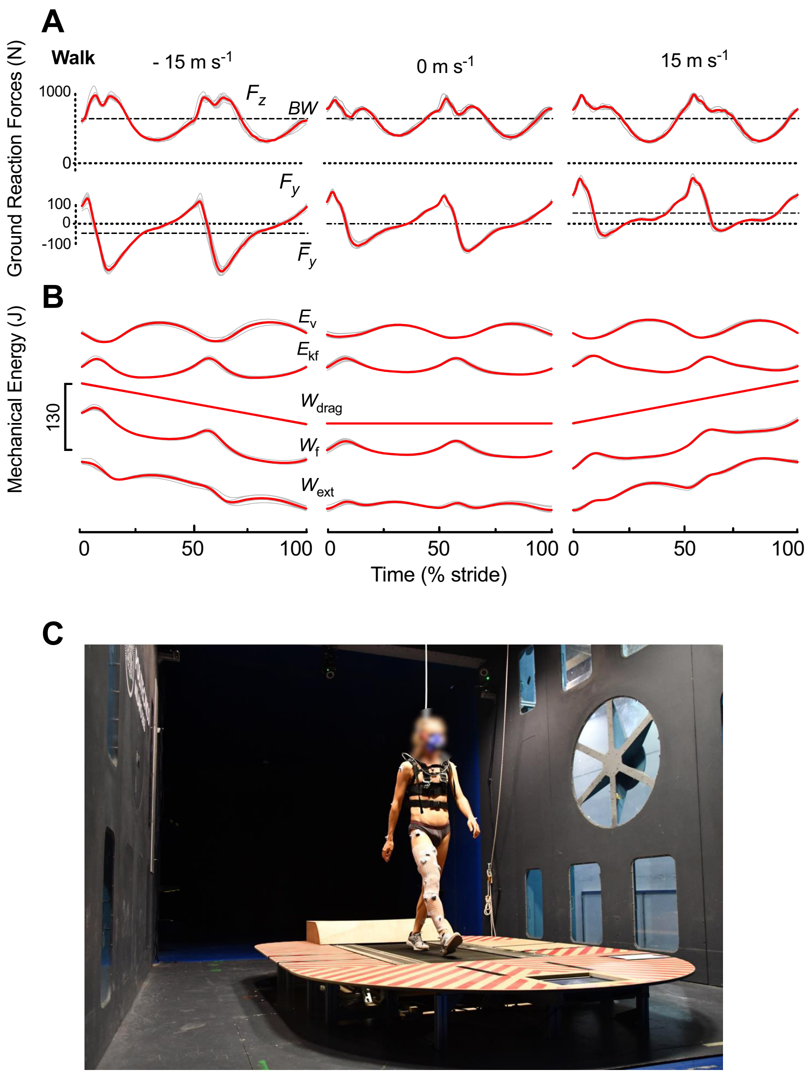

Figure 2. *A*: typical traces of the vertical (F_z) and fore-aft (F_y) component of the GRF as a function of time (in %stride period) of 1 subject (mass: 64 kg; height: 1.75 m) walking at 1.5 $m{\cdot}s^{-1}$ with a tailwind speed of -15 $m{\cdot}s^{-1}$, without a wind force, and with a headwind speed of 15 $m{\cdot}s^{-1}$. The gray traces represent all strides recorded during 1 trial normalized in %stride, and the red line represents the average of all strides. When the subject is not on the treadmill, F_z and $F_y = 0$ (dotted line). The dashed horizontal lines represent the average ground reaction forces when the subject walks or runs on the treadmill: in the vertical direction, this line corresponds to the subject's body weight (BW), whereas in the fore-aft direction the dashed line ($\overline{F}_y$) corresponds to the opposite of the drag force ($\overline{F}_d$). *B*: mechanical energy of the center of mass (CoM; in J) from the same traces as in *A*. From *top* to *bottom*: E_v, is the energy due to the vertical movements of the CoM, E_{kf} is the energy due to the changes in its fore-aft velocity, W_{drag} is the work done by the subject against the wind, W_f is the work done to sustain the fore-aft movements of the CoM ($W_f = E_{kf} + W_{drag}$), and W_{ext} is the work done to sustain the progression of the CoM in the wind ($W_{ext} = E_v + W_f$). *C*: picture of a subject walking in the wind tunnel (here without wind) on the instrumented treadmill setup designed to reduce turbulence around the runner.

and ended when the contralateral foot touched the ground (the instant before $F_z > 30$ N) (18, 36).

Acceleration, velocity, and vertical displacement of the CoM.

Calculations for the acceleration, velocity, and displacement of the CoM were done as in Gosseye et al. (37), Mesquita et al. (17), and Dewolf et al. (26) and will, therefore only be briefly explained here. The lateral component of the GRF was not considered since its contribution to the external work is negligible (2, 38).

When moving in the wind on the level, the following forces were applied to the body: the body weight (BW), the GRF (F), and the drag (F_d). In this case, over an integral number of strides, the average fore-aft GRF ($\overline{F}_y$) was equal and opposite to F_d and the average vertical GRF ($\overline{F}_z$) was equal to BW.

The acceleration of the CoM in the fore aft (a_y) and vertical (a_z) directions relative to a fixed reference frame attached to the wind tunnel was given as: $a_y = \frac{F_y - \overline{F}_y}{m}$, and $a_z = \frac{F_z - \overline{F}_z}{m}$, where m is the body mass. A time-integration of the a_y and a_z curves by the trapezoidal method gave the fore-aft and vertical velocity changes of the CoM plus their respective integration constants (34, 39).

To be included in the study, the strides had to fulfill the two following criteria, as in Dewolf et al. (27): *1*) the average vertical force during a complete stride ($\overline{F}_z$) had to be within 10% of BW; and (*2*) the sum of the increments and sum of the decrements of the instantaneous CoM fore-aft velocity had to differ less than 25%. In total, between 13 and 84 strides were analyzed per condition and per subject. A total of 8,850 strides were analyzed (5,443 strides for the running trials and 3,307 strides for the walking trials, i.e., 1,111 ± 68 strides per subject, mean ± SD).

External mechanical work.

The external power ($\dot{W}_{ext}$) developed during each step by the forces applied to the body was computed as the algebraic sum of the power developed by the GRF ($\dot{W}_{com}$), plus the power developed to counter the drag ($\dot{W}_{drag}$). From these, the time integral of $\dot{W}_{com}$ and $\dot{W}_{drag}$ give, respectively, the work done to sustain the movements of the CoM (W_{com}) and work done against the drag (W_{drag}). The sum of W_{com} and W_{drag} gives the external work, W_{ext}, similar to the methods proposed in Ref. 17.

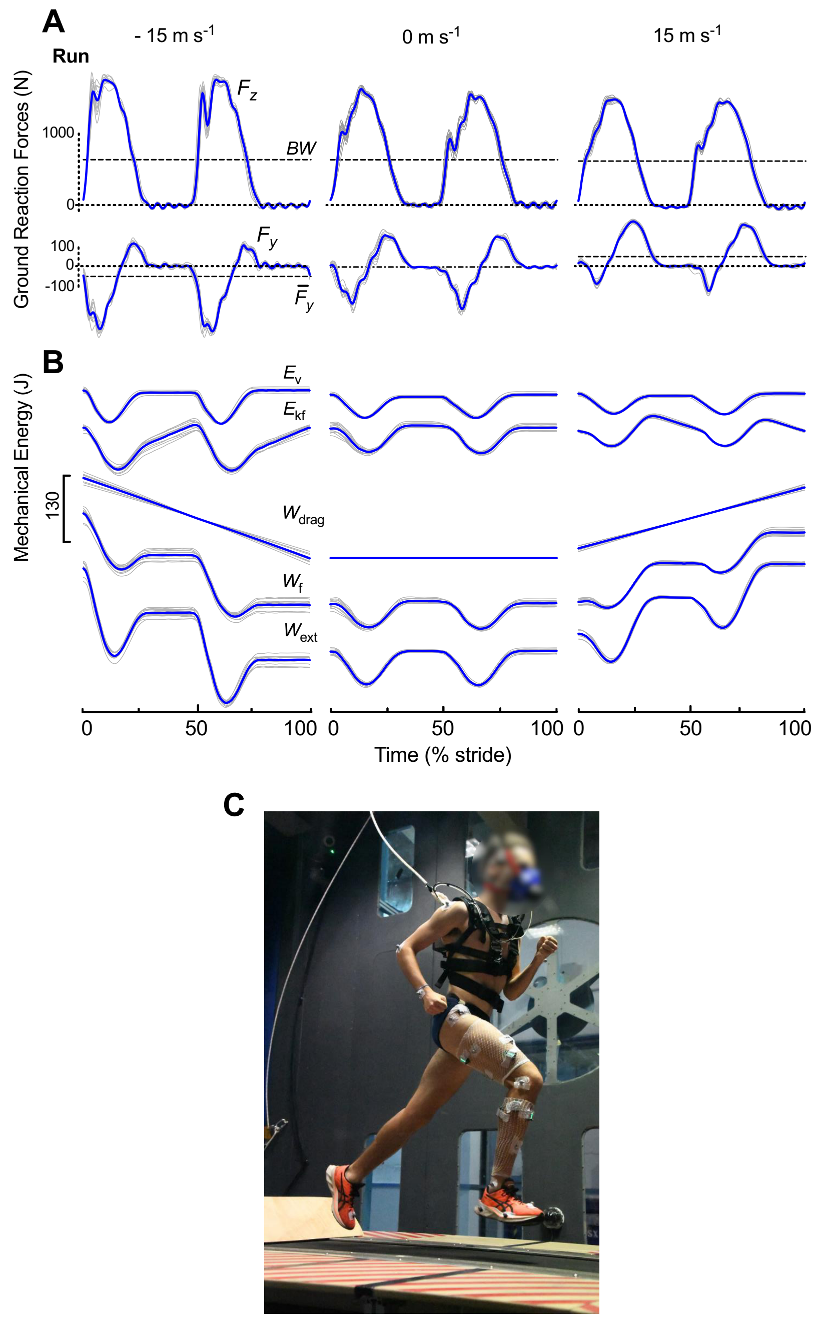

Figure 3. *A*: typical traces of the vertical (F_z) and fore-aft (F_y) forces of 1 subject (mass: 64 kg; height: 1.75 m) running at 4.5 m·s^{-1} without a wind force and with tail and headwind speeds of ±15 m·s^{-1} (tail: –; head: +). The gray traces represent all strides recorded during 1 trial normalized in %stride, and the red line represents the average of all strides. When the subject is not on the treadmill, F_z and F_y = 0 (dotted line). The dashed horizontal lines represent the average ground reaction forces when the subject walks or runs on the treadmill: in the vertical direction, this line corresponds to the subject's body weight (BW), whereas in the fore-aft direction the dashed line ($\overline{F}_y$) corresponds to the opposite of the drag force ($\overline{F}_d$). *B*: mechanical energy of the center of mass (CoM; in J) from the same traces as in *A*. From *top* to *bottom*: E_v, is the energy due to the vertical movements of the CoM, E_{kf} is the energy due to the changes in its fore-aft velocity, W_{drag} is the work done by the subject against the wind, W_f is the work done to sustain the fore-aft movements of the CoM ($W_f = E_{kf} + W_{drag}$), and W_{ext} is the work done to sustain the progression of the CoM in the wind ($W_{ext} = E_v + W_f$). *C*: picture of a subject running in the wind tunnel against a headwind.

The two first curves of Figs. 2*B* and 3*B* represent typical traces of the energy done to sustain the fore-aft and vertical movements of the CoM, respectively, E_{kf} and E_v, during one stride of walking and one stride of running, computed as in Refs. 2, 40. The middle curves of Figs. 2*B* and 3*B* represent W_{drag}, the work done by the subject on the wind:

$$W_{drag} = \int_{t_1}^{t_2} \overline{F}_y v_{belt}\, dt. \tag{1}$$

When moving against a wind force, the work (W_f) was done during the contact phase to sustain the kinetic energy changes of the CoM but also to counteract the drag:

$$W_f = E_{kf} + W_{drag}. \tag{2}$$

The bottom curve represents the external energy of the CoM, which was computed as the sum of the E_v and E_{kf} curves plus the curve W_{drag}.

$$W_{ext} = E_v + E_{kf} + W_{drag}. \tag{3}$$

Positive (W_f^+, W_v^+, and W_{ext}^+) and negative (W_f^-, W_v^-, and W_{ext}^-) work were computed by respectively summing the increments and the absolute value of the decrements of the W_f, E_v, and W_{ext} curves, respectively. An in-depth description of the method is available in the supplementary materials.

Aerodynamic parameters.

The drag applied to a subject, F_d, is dependent on the drag area, C_dA, i.e., the projected frontal area of the subject (A)

multiplied by the drag coefficient (C_d) and by the dynamic air pressure of the moving air stream (q) (4, 5, 7, 8). As the subject moved at constant speed, the magnitude of the average fore-aft ground reaction force ($\overline{F}_y$) computed over an integral number of strides was equal to $|F_d|$. Consequently, the C_dA of the subject was given as:

$$C_dA = \frac{\overline{F}_y}{q}. \quad (4)$$

In turn, q could be evaluated as the kinetic energy per unit volume of a moving solid body $q = 0.5\,\rho\,u^2$, where ρ was the air density and u the wind speed. In turn, the air density ρ was computed by $\frac{p}{RT}$, where p is the static air pressure, R is the gas constant, and T is the air temperature. The instantaneous values of these variables (u, q, p, and T) were recorded at 1 kHz during trials. Wind speed, u, deviated from the nominal wind speed on average by 2 ± 0.4% over all trials. The average wind speed, U, was similar between walking and running ($F = 1.14$, $P < 0.344$), air density was on average at 1.137 ± 0.005 kg·m^{-3}, and the average temperature was 28.3 ± 1.3°C (301.54°K) over all trials.

Percent recovery, drag ratio, and phase lag.
Energy transduction between the W_f and E_v curves in both walking and running were assessed by the percent recovery (%recovery) as in Ref. 31. The drag ratio (D_r) was obtained by dividing the work done to overcome drag (W_{drag}) by the external work (W_{ext}).

$$D_r = \frac{w_{drag}^{+/-}}{W_{ext}^{+/-}}, \quad (5)$$

In the case of headwind, the D_r was the ratio between the sum of the positive increments whereas in the case of tailwind, the negative increments were used.

The phase ϕ, expressed in degrees, evaluated the lag between the maximum of $W_f(t_f)$ and the minimum of $E_v(t_v)$ in walking and between the minimum of $W_f(t_f)$ and the minimum of $E_v(t_v)$ in running:

$$f = 360\frac{t_f - t_v}{ST}. \quad (6)$$

where ST is the step period.

Statistics

For each participant, the different variables were first averaged across the right and left steps for each stride then averaged per stride. Descriptive statistical analyses were performed. First, a Shapiro-Wilk test was performed to verify normality. Then, a linear mixed effect model assessed the effect of wind speed on the calculated variables. Depending on the lowest Akaike Information Criterion either U or U^2 was used for the wind effect. For each comparison, the F and P values for the fixed effect are reported. To analyze eventual differences in the aerodynamic variables between walking and running, all data were pooled together and the effect of wind, walking/running speed, and their interaction were analyzed. Statistical tests were run on IBM SPSS Statistics (PASW Statistic 27). The results of the statistical tests were considered significant for a P value <0.05.

RESULTS

Drag as a Function of Wind Speed

As wind speed increases, the magnitude of the drag $|F_d|$ increased (Fig. 4A) both in walking ($F = 1195.02$, $P < 0.001$) and in running ($F = 1317.03$, $P < 0.001$). However, at a given wind speed, the drag $|F_d|$ was greater in walking than in running ($F = 92.56$, $P < 0.001$), and this difference was marked at the fastest wind speeds (regression curve of $|F_d|$ as a function of the instantaneous wind speed u, for running: $|F_d| = 0.85 - 0.108\,u + 0.239\,u^2$, $r^2 = 0.986$ and for walking: $|F_d| = 0.635 + 0.055\,u + 0.265\,u^2$, $r^2 = 0.986$) (95% confidence intervals show difference between walking and running for headwinds ≥10 m·s^{-1}). Note also that similar trends were observed for the F_d versus U relation for both head- and tailwinds (Supplemental Table S1).

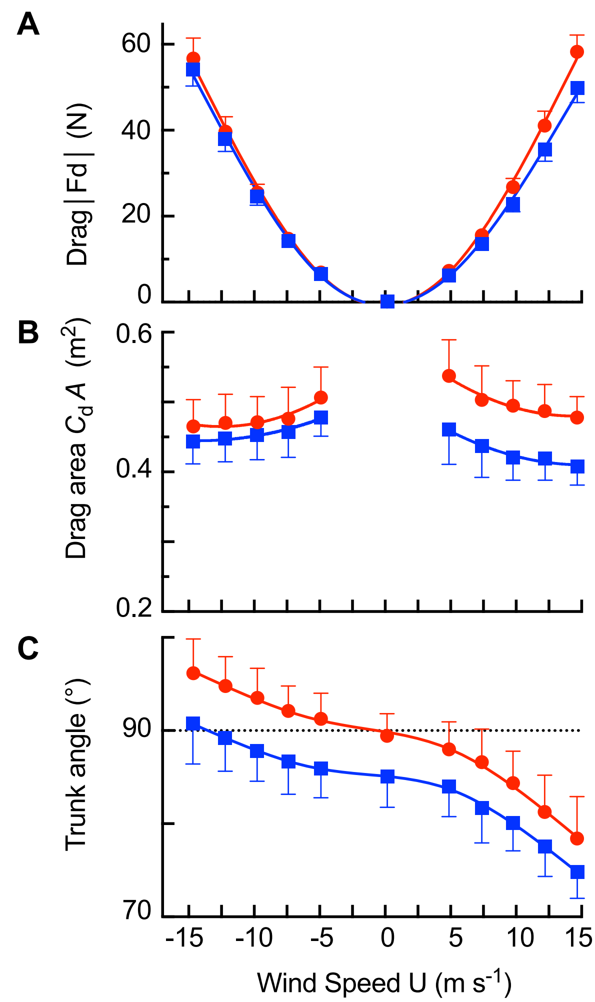

Figure 4. Aerodynamic variables in walking (red circles) and running (blue squares) as a function of wind speed (U in m·s^{-1}). *A*: magnitude of drag (in N) in both walking and running. *B*: drag area (C_dA) is computed from *Eq. 4*. No values are expressed when wind speed is nil, since in *Eq. 4*, the wind speed U is part of the denominator and C_dA mathematically tends toward infinity when the wind speed tends to zero. *C*: trunk angle (expressed in degrees) in walking and running. In *A–C*, the points are the average of the data measured on all steps of all subjects. The vertical bars indicate the standard deviation of the mean and are drawn when they exceed the size of the symbol. Filled and dashed lines are spline functions with 4 notches from all data points. These data are plotted via Graphpad Prism 10 (GraphPad Software, Boston, MA).

The dynamic air pressure (q) increased with the square of wind speed and was not different between head- and tailwinds (post hoc test always equal $P = 1$ between equivalent head- and tailwind speeds; regression curve for running: $q = -0.03 - 6.9610^{-4}\ u + 0.578\ u^2$, $r^2 = 0.999$ and for walking: $q = -0.03 - 4.45\ 10^{-5}\ u + 0.578\ u^2$, $r^2 = 0.999$). The C_dA decreased as a function of increasing wind speed (Fig. 4B) both in walking ($F = 6.25$, $P < 0.001$) and in running ($F = 23.89$, $P < 0.001$). With headwind, C_dA was greater in walking than in running (post hoc effect between +5 and +15 m·s^{-1}, $P < 0.001$). On the contrary with tailwinds faster than −5 m·s^{-1}, there was no significant difference between the two gaits (post hoc between −7.5 and −10, −12.5, and −15, $P = 1$). Without wind, the trunk was vertical during walking and slightly leaned forwards (5°) during running (Fig. 4C). Both in walking and in running, the trunk tilted forward (≈11° for both) with headwind and backward (≈5° for both) with tailwind ($F = 112.77$, $P < 0.001$ for running and $F = 217.61$, $P < 0.001$ for walking).

Step Length and External Work While Walking and Running in the Wind

Wind speed had a significant effect on the step length (Supplemental Fig. S2) both in walking ($F = 8.13$, $P < 0.001$) and in running ($F = 14.98$, $P < 0.001$). In walking, step length decreased by ∼5% when comparing no wind and −15 m·s^{-1} (post hoc $P < 0.001$). Conversely, in running step length decreased with increasing headwind ($P < 0.001$ between 15 m·s^{-1} and no wind).

The magnitude of the work done to overcome wind resistance ($|W_{drag}|$) is presented in Fig. 5C. The muscle-tendon units did positive work against headwind and negative work against tailwind. In both directions, $|W_{drag}|$ increased with wind speed ($F = 4134.44$ in walking and $F = 1360.72$ in running, $P < 0.001$). Note also that when normalized by distance traveled, W_{drag} was slightly greater in walking than in running ($F = 3.01$, $P < 0.001$).

When walking or running in the wind, since the subject is moving on level ground, $W_v^+ \approx W_v^-$ (Figs. 2, 3, and 5A). However, in walking both W_v^+ and W_v^- increased as wind speed increased (W_v^-: $F = 35.32$, $P < 0.001$; W_v^+: $F = 35.32$, $P < 0.001$), whereas the effect of wind on either variable was much smaller in running (W_v^-: $F = 8.85$, $P < 0.001$; W_v^+: $F = 8.88$, $P < 0.001$).

In both gaits, head- and tailwind speed influenced the positive (W_f^+) and negative (W_f^-) work done to move the CoM forwards (for W_f^+: $F = 867.45$ in walking and $F = 1034.28$ in running, $P < 0.001$ and for W_f^-: $F = 1643.28$ in walking and $F = 1005.77$ in running, $P < 0.001$). As compared to walking and running with no wind, when headwind increased, W_f^- decreased, while W_f^+ increased (Fig. 5B). Conversely, with a

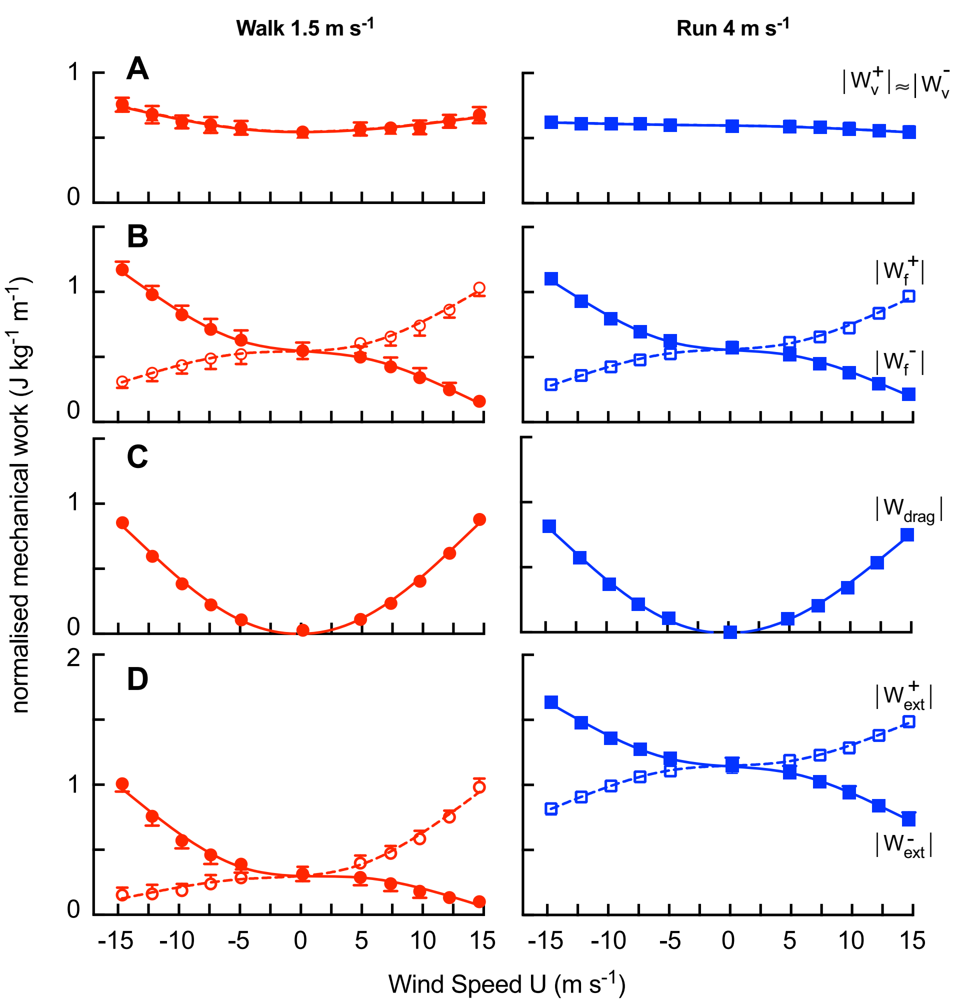

Figure 5. Magnitude of the mass-specific mechanical work per unit distance (J·kg^{-1}·m^{-1}) in walking (red circles) and running (blue squares) as a function of the average wind speed (U). Open symbols represent positive work (superscript +) and closed symbols, negative work (superscript −). *A*: W_v is the work done to sustain the vertical movements of the center of mass (CoM). *B*: W_f is the work the sum of the work done to sustain its fore-aft movements of the CoM plus the work done against the wind. *C*: work done against the wind. *D*: external work (W_{ext}) done to maintain the movements of the CoM relative to the surroundings. In *A*–*D*, the points are the average of the data measured on all steps of all subjects. The vertical bars indicate the standard deviation of the mean and are drawn when they exceed the size of the symbol. Filled and dashed lines are spline functions with 4 notches from all data points. These data are plotted via Graphpad Prism 10 (GraphPad Software, Boston, MA).

tailwind, W_f^- increased with wind speed whereas W_f^+ decreased. In both gaits, the net increase in W_f (i.e., $|W_f^+ - |W_f^-||$) was about equal to $|W_{drag}|$ (Fig. 5C).

In walking as in running, the effect of wind on W_{ext}^+ and W_{ext}^- was similar to the one observed on W_f^+ and W_f^- (Figs. 2, 3, and 5D), meaning that W_{ext}^+ increased with faster headwinds and decreased with faster tailwinds ($F = 388.01.45$, $P < 0.001$), whereas W_{ext}^- decreased with increasing headwinds and increased with increasing tailwind ($F = 547.11$, $P < 0.001$). Note that in both gaits, the duration of the positive work phases (t_{push}) increased when the headwind speed increased and decreased when tailwind speed increased. Inversely, the duration of the negative work phases decreased when the headwind speed increased and increased when tailwind speed increased (see Supplemental Fig. S3).

%*Recovery*, Drag Ratio and Phase Shift between W_f and E_v

The drag ratio ($D_r = \frac{W_{drag}}{W_{ext}}$) increased as a function of wind speed in both walking and running (in walking: $F = 536.03$, $P < 0.001$, in running: $F = 1148.70$, $P < 0.001$). This increase was greater in walking than in running as evidenced by the interaction effect observed between wind speed and moving speed ($F = 26.74$, $P < 0.001$) (Fig. 6A).

In both gaits, wind had a significant effect on the phase shift (ϕ) between the minimum of W_f and the maximum of E_v in walking ($F = 97.95$, $P < 0.001$) and the minima of both W_f and E_v in running ($F = 434.78$, $P < 0.001$) (Fig. 6B). Without wind, ϕ was close to 0° when walking (phase opposition) at 1.5 m·s^{-1} and when running at 4 m·s^{-1} (in phase). In walking, the W_f and E_v curves were perfectly out of phase ($\phi = 0°$) with a tailwind of ~5 m·s^{-1}. When the tailwind decreased and became a headwind, the lag between the two minima increased. When the tailwind became greater than ~5 m·s^{-1}, the lag between the two minima was reduced.

In running, the W_f and E_v curves were perfectly in phase (i.e., $\phi = 0°$) with a headwind of ~10 m·s^{-1}. When the headwind increased, the minimum of E_v occurred later than the minimum of W_f. On the contrary, if the headwind slowed or if the tailwind got faster, the minimum of E_v occurred before the minimum of W_f.

In walking, when wind speed increased the %recovery decreased ($F = 26.02$, $P < 0.001$) (Fig. 6C). The %recovery was at its peak at 0 m·s^{-1} and followed a curvilinear decrease with both head- and tailwinds. In running, %recovery increased with increasing wind speed ($F = 65.05$, $P < 0.001$) principally with tailwinds (post hoc between 0 wind and all tailwind speeds $P < 0.001$). Against headwinds, the %recovery at 0 wind significantly differed only at +15 m·s^{-1} (post hoc $P < 0.001$) (Fig. 6D).

DISCUSSION

In the present study, we analyzed the effects of wind (ranging from −15 to +15 m·s^{-1}) on the external work (W_{ext}) and on the mechanics of locomotion when walking at 1.5 m·s^{-1} and running at 4 m·s^{-1}. In this section, we will first discuss how aerodynamic variables change during human locomotion against head- and tailwinds. We will then analyze how the ratio between negative and positive work, the drag ratio, and the phase lag change with increasing wind. Then, we will consider practical implications of our results and compare these to two situations where the ratio between negative and positive work is imbalanced: moving against tractive forces and moving on a slope.

Aerodynamics of Walking and Running in the Wind

While the study of locomotion against wind forces is not novel (5, 7, 11, 15), the direct measurement of drag via the GRF is innovative. This method was based on the following principle:

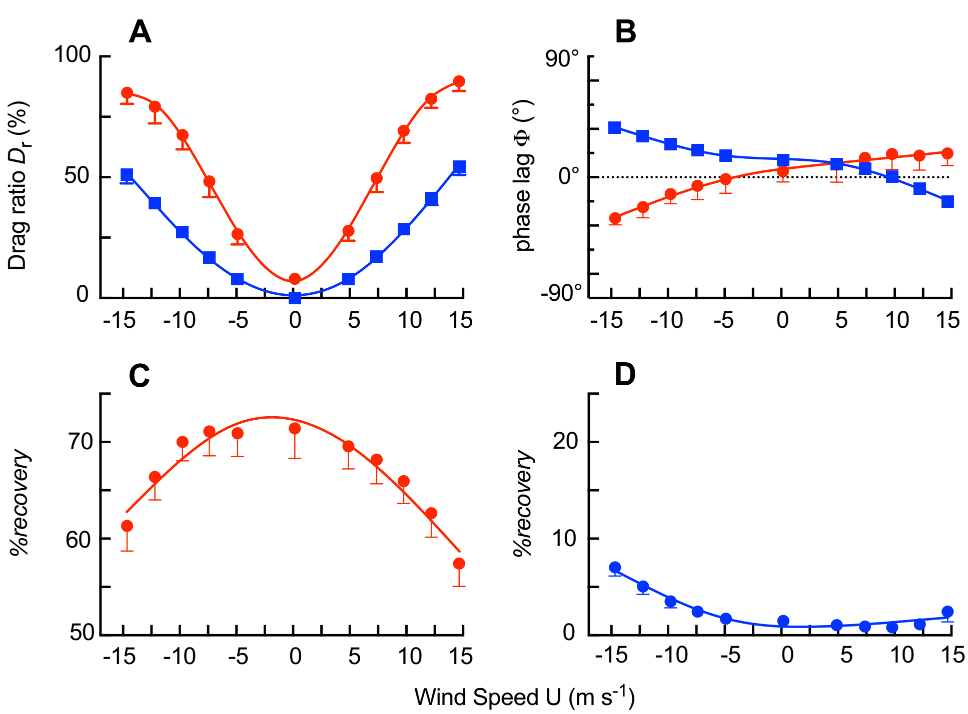

Figure 6. Drag ratio, D_r (*A*), and phase lag, ϕ (*B*), in walking and in running as a function of wind speed (*U*). Energy recovered through energy transduction between W_f and E_v (%recovery) as a function of the wind speed in walking (*C*) and in running (*D*). In *A*–*D*, the points are the average of the data measured on all steps of all subjects. The vertical bars indicate the standard deviation of the mean and are drawn when they exceed the size of the symbol. Filled and dashed lines are spline functions with 4 notches from all data points. These data are plotted via Graphpad Prism 10 (GraphPad Software, Boston, MA).

when the average speed of progression does not change over an integral number of strides, the average fore-aft acceleration of the CoM is nil and the magnitude of the average fore-aft component of the GRF is equal to the drag force.

In the present study, we assumed that the drag remained constant during the stride. In other words, we considered that the movements of the limbs during the stride (the turbulence of which is often referred as "Active Drag") do not significantly change the projected frontal area of the subject. This assumption was also made by Pugh (8) and Davies (5). In fact, the positioning of the limbs generates little variation of C_dA (9, 16). Similar observations were made in cycling where the pedaling motion of the lower limbs has negligible effect on the C_dA (41).

With increasing wind speeds, the drag force exhibits a quadratic rise, reaching ~50–60 N at the highest wind speeds (Fig. 4). These results are similar to the CFD simulations of Schickhofer and Hanson (9), who obtain a drag force of 18.45 N at 10 $m \cdot s^{-1}$, compared to our experimental result of 22.4 N. When wind speed increases further, i.e., at 15 $m \cdot s^{-1}$, slight differences appear in F_d between walking and running. Furthermore, when applying Davies' equation to estimate the projected area, our results for C_d vary between 0.89 and 1.05 similar to previously documented values (5, 8, 21).

Given the similar average wind speed and consistent air density of 1.137 $kg \cdot m^{-3}$ ± 0.005 $kg \cdot m^{-3}$ across all trials, the observed difference in F_d can be attributed solely to a change in C_dA, which decreases more with increasing wind velocities in running than in walking (Fig. 4 and Supplemental Table S1). In turn, this difference in C_dA between the two gaits may be attributed, at least partially, to the more forward-leaning posture of the trunk, which reduces the projected frontal area of the runner. Furthermore, this increased trunk flexion, associated with shorter steps and higher step frequency (Supplemental Fig. S2), is a trait generally associated with initial CoM acceleration (42), decreased push averaged power (34, 43) and is related to running economy and performance (44–47). Van Oeveren et al. (47) explained that a greater trunk lean likely increases propulsion, tilts the GRF vector further, and shifts the center of mass forward. Nonetheless, running performance is typically associated with a more upright trunk posture, whereas novice runners, especially when fatigued, tend to lean their trunks more. Furthermore, increased trunk lean, due to its role on the pelvis, is linked with several running injuries (48, 49).

Improving aerodynamics during walking and running has received little attention in sports science, as it would not lead to major improvements in performance. However, aerodynamics are rather important in sports such as speed skating and cycling where speeds, and hence drag forces, are greater (10). However, when the limits of performance are nearly reached, even small changes can improve running time (50). Indeed, in the past 20 years, the marathon record has improved by 3.6% between Paul Tergat's 2:04:55 and Kelvin Kiptum's 2:00:35. For example, although hypothetical, decreasing drag by drafting behind another athlete decreases the drag coefficient (C_d) by 9.7%, potentially saving up to 535 s over an entire marathon run at 4.7 $m \cdot s^{-1}$ (21). Note that this improvement will be speed and distance between runner dependent (8, 9, 13, 16, 22). In light of this, we would argue that before modifying one's gait, elite athletes should look at improving their drafting technique [e.g., by improving racing strategy (51) and adapted clothing (52)].

Positive and Negative External Work, Drag Ratio, and Phase Lag While Walking and Running in the Wind

Headwinds impede forward progression. Therefore, to maintain the average speed of progression constant from one stride to the next, $W_f^+ > W_f^-$ and $W_{ext}^+ > W_{ext}^-$ (Figs. 2, 3, and 5). Conversely, tailwinds aid forward progression and $W_{ext}^- > W_{ext}^+$. Additionally, in walking when head- or tailwind increases, W_v increases. This could be explained by the drag generating a lift force accelerating the CoM upwards, at certain moments of the stride, and thus increasing the vertical motion of the CoM (5). In running, the vertical movements of the CoM are slightly reduced at the fastest headwind speed as compared to running without wind. When running against fast headwinds, Davies (5) reports that subjects "lean" on the wind flow and tuck their head in, reducing the vertical movement of the CoM. Consistently, our measurements show a ~12% increase in the forward trunk inclination at the fastest wind speed.

When walking in the presence of increasing headwind, due to W_{drag}, the angle ϕ becomes greater than 0°, showing that the minimum of W_f occurs later in the step than the minimum of E_v. As a result, the periods during which the W_f and E_v curves increase together becomes longer and the percentage of energy transduction (%recovery) between energy W_f and E_v, decreases from 65% to 55% (Fig. 6, *C* and *D*). In the presence of increasing tailwind, the angle ϕ decreases and becomes smaller than 0°, demonstrating that the minimum of W_f occurs earlier in the step than the minimum of E_v. As a result, the periods during which the W_f and E_v curves decrease together becomes longer and the %recovery decreases from 65% to 55% (Fig. 6, *C* and *D*). When running in presence of increasing headwind, the angle ϕ decreases and becomes smaller than 0°, showing that the periods during which the W_f curve increases while the E_v curve decreases and gets longer, allowing energy transduction between the two curves. In the presence of increasing headwind, the angle ϕ becomes greater than 0°, showing that the periods during which the W_f curve decreases while the E_v curve increases, allowing for energy transduction between the two curves. Therefore, when ϕ deviates from 0° (in both directions), the %recovery increases slightly (Fig. 6, *C* and *D*).

Effect of the Wind on the Drag Ratio

When walking or running on a treadmill, humans move through still air, which offers negligible resistance to their forward motion. Consequently, the product of the drag times the distance covered is small as compared to the total muscular work done to move the body, and the drag ratio, $D_r = \frac{W_{drag}}{W_{ext}}$, is close to zero (Fig. 6*A*). On the contrary, in fast winds, the drag ratio, increases up to ~80% of W_{ext} in walking and ~50% in running (Fig. 6*A*), suggesting that the fraction of work done against the environment increases if the medium crossed offers a greater resistance/assistance to forward motion. However, with increasing wind speed, the ratio between $|W_{ext}^-|$ and W_{ext}^+ deviates from 1.0, and with it, a reduction of the energy-saving pendular mechanism of walking and bouncing mechanism of running is observed (Fig. 6, *C* and *D*). This has been observed in other situations (5, 25, 53). We also observed that both in walking and in running, the duration of the push phase (t_{push}, i.e., the duration of the positive work production) increases when the headwind speed increases whereas the duration of the brake phase (t_{brake}) increases when the tailwind speed increases (Supplemental Fig. S3). This increase in t_{push} when running against the wind and of t_{brake} when running with the wind reduces the average positive power developed during the positive/negative work phase, respectively.

Furthermore, an increase in D_r together with the imbalance in the positive/negative external work could modify the overall efficiency of locomotion (25, 54). Indeed, against drag forces generated by wind, the "apparent" efficiency decreases toward efficiencies observed in slope running (5). Note that this last study, based on three subjects, showed considerable variability in their data, mostly due to subject heterogeneity and to the small sample size. Also, those results are affected by the included determinants of the total mechanical work and its apparent nature due to elastic contribution of tendons, which is small in walking but considerable in running (3, 29, 30, 55–57). The effect of D_r on the efficiency of locomotion could be tested by *1*) measuring the internal and thus the total muscular work done during locomotion in the wind, and *2*) evaluating the energy expenditure during walking and running with head and tail winds blowing at the same speed.

Practical Considerations about the Mechanics of Wind Locomotion

Transposing locomotion in the wind tunnel to overground locomotion.

Note that when walking or running on the ground instead of a treadmill, the "apparent wind" speed, as known in sailing (58) should be corrected to the "true wind" speed; the wind that the subject experiences while moving. For example, running on the treadmill at 4 $m \cdot s^{-1}$ with a headwind of 15 $m \cdot s^{-1}$ corresponds to running on the ground at 4 $m \cdot s^{-1}$ with a true wind of 11 $m \cdot s^{-1}$. Moreover, running on the ground at 4 $m \cdot s^{-1}$ with a tailwind of 4 $m \cdot s^{-1}$ corresponds to running on the treadmill with no wind. When simulating overground locomotion, using a treadmill in a wind tunnel, both with head- and tailwinds, the speed of the belt should be subtracted from the wind speed to match ecological conditions. This concept should be acknowledged when transposing our findings to field tests, such as drag formations (13, 14, 16, 18, 21, 22).

Comparison to locomotion on a slope.

Previous studies have shown, both in walking (26) and in running (17), that the W_{ext} while moving on a slope of n% ($0\% < n < 15\%$) (27, 28) is equivalent to W_{ext} while moving on the level with a horizontal tractive force representing n% of BW. From a metabolic standpoint, similarities have been documented between walking-running with head and tailwind and walking-running uphill and downhill (5); however, no consensus exists (8). When moving in the wind, if the drag is expressed as a percentage of BW or as a function of squared wind speed, we observe similarities between the magnitude of the drag and both the equivalent slope (27, 28) and the magnitude of tractive force (17, 26) in both types of locomotive strategies. For an in-depth discussion on the matter, the reader is invited to consult the supplementary materials (Supplemental Figs. S4 and S5).

Inclining the treadmill by 1% compensates for the lack of air resistance.

Jones and Doust (59) proposed that to (metabolically) compensate for the lack of air resistance during treadmill running, researchers should incline a treadmill by 1% to be able to compare their results to overground running. Despite the paper's popularity, systematic reviews like those of Miller et al. (60) and Van Hooren et al. (61), have shown that during efforts below 18 $km \cdot h^{-1}$, no difference in oxygen consumption is observed between level treadmill and overground running. The last authors explain that as air resistance increases with the square of wind speed, when running at high speeds the overground $\dot{V}O_2$ more closely matches treadmill running with a 1% incline. Based on the regression curve for $|F_d|$ presented in our results, at the speeds covered in Jones and Doust (59), a 66-kg person (the average subject mass in the present study) running at 2.92 $m \cdot s^{-1}$ would experience a "true" drag force of 2.36 N, corresponding to an incline 0.36% (62, 63). At 5 $m \cdot s^{-1}$ the drag is at 6.07 N (corresponding to 0.93% incline). Supplemental Figure S6 shows the increase in drag, expressed in %BW, as a function of running speed.

Running records in sprint races are not considered with wind speeds above 2 $m \cdot s^{-1}$.

Based on the quadratic nature of wind and drag, winds of ~2 $m \cdot s^{-1}$ would have little impact on road races; however, when running speed is much higher (~10 $m \cdot s^{-1}$ for an elite sprinter compared to 5.8 $m \cdot s^{-1}$ for an elite marathoner) even small changes in wind speed have an important effect on the drag as is the case in faster sports such as cycling or speed skating.

Per World Athletics Competition Rule 31.14.3 (64): "For performances made outdoors up to and including 200 m [...] if the wind velocity, measured in the direction of running, averages more than 2 meters per second, the performance will not be ratified." When we apply our findings to Usain Bolt's record average speed of 10.43 $m \cdot s^{-1}$ (65), the drag force in a system with no wind would be ~25.5 N, ~2.7% of Bolt's 94 kg (Bolt's projected frontal area is not considered). Supposing that Bolt had run with an added 2 $m \cdot s^{-1}$ tailwind to the system, his drag would have been of 16.7 N (1.8% of BW) for a resultant wind speed of 8.43 $m \cdot s^{-1}$. Assuming Bolt maintains the same total mechanical power (~50 $W \cdot kg^{-1}$) (66), we can approximate an increase of 1.9% in running speed (*Supplemental Eq. Se3*).

Perspective for future research based on comparable methods.

Wind tunnel studies are rather useful in understanding the relationship between the drag force applied to a runner and wind speed, based on the biomechanical adjustments of the drag area. However, wind tunnel testing requires substantial time and resources, and therefore, cost-effective alternatives have been used to advance research without necessarily relying on the former, such as computational fluid dynamics (CFD) simulations or tractive devices that hinder/aid progression. For example, in the study of Da Silva et al. (18), the gross metabolic power was calculated when running against tractive forces ranging from 0 to 8 N, which simulated running against impeding air resistance. The authors justified this range based on several CFD studies, which estimated that drag forces on elite marathoners were between 6.6 and 7.94 N (9, 13, 22). Based on our results, elite marathoners running at the official marathon record speed of 5.83 $m \cdot s^{-1}$ experience a drag of ~8.1 N (~1.4% of BW for Eliud Kipchoge's 58 kg), a comparable result. Therefore, even if the kinematic intricacies of locomotion in the wind are difficult to capture using such cost-effective alternatives, they provide results that may be of interest to sports scientists.

Limitations

As the time required to match the nominal wind speed once changed was long, trials were only randomized by wind speed. This experimental protocol may have incurred fatigue and habituation bias to our results. Furthermore, although our sample size was decided based on a power analysis, timing, and funding constraints, it nevertheless remains small and composed of only male subjects. Thirdly, the subjects in our study are all professional or semiprofessional athletes, which is interesting when comparing our results to those of Pugh (7) and Davies (5) who both had experienced runners in their studies. However, in the studies of mechanical changes in slope locomotion (27, 28) and against tractive forces (17, 26) the subjects recorded were recreational runners making direct comparisons more difficult. Finally, the method used here does not allow us to measure the individual limb GRF*s* during walking's double contact phase, which is possible, among others with a split-belt treadmill. Therefore, one cannot directly calculate the simultaneous work done by each limb during the walking step-to-step transition (67).

Conclusions

In conclusion, our findings expand our understanding of the interaction between wind and the biomechanics of human locomotion. Wind increases external work, alters the balance of positive/negative work, and adjusts the subject's C_dA. Locomotion in the wind shares similarities with walking and running on slopes or with a tractive force, albeit with the external force distributed across the frontal area of the body. This study offers insights for optimizing performance, particularly in running, potentially aiding in breaking the official 2-h marathon barrier. Moreover, understanding how gait is modified against external forces furthers our understanding of how one adapts the two fundamental locomotion mechanisms and provides part of the puzzle for understanding locomotor efficiency changes.

GLOSSARY

A	Projected frontal area facing the airflow
a_y, a_z	Fore-aft and vertical components of the acceleration of the CoM
BW	Body weight
C_d	Drag coefficient
C_dA	Drag area: drag coefficient multiplied by the projected frontal area facing airflow
CoM	Body center of mass
D_r	Work done to overcome the drag over the external work done
E_{kf}	Kinetic energy done to sustain the fore-aft motion of the center of mass
E_v	Energy due to the vertical motion of the center of mass
F	GRF vector
F_d	Aerodynamic drag force
F_x, F_y, F_z	Lateral, fore-aft, and vertical ground reaction forces
$\overline{F}_y$	$\overline{F_z}$ Average fore-aft and vertical ground reaction forces
GRF	Ground reaction force
MTU	Muscle-tendon unit
q	Dynamic air pressure
u	Instantaneous wind speed
U	Average wind speed
W_{com}, $\dot{W}_{com}$	Work and power done to sustain the movements of the CoM
W_{drag}	Work required to overcome the resistance of the medium
W_{ext}, $\dot{W}_{ext}$	External work and power done to sustain the movements of the center of mass and do work against the environment
W_f	Work done by the muscle-tendon units to sustain the kinetic energy changes of the CoM and counteract the drag
W_f^+, W_v^+, W_{ext}^+	Positive work values done by summing the increments of each respective variable
W_f^-, W_v^-, W_{ext}^-	Negative work values done by summing the absolute value decrements of each respective variable
W_{int}	Work done to move the upper and lower limbs relative to the CoM
W_{tot}	Total mechanical work done ($W_{tot} = W_{ext} + W_{int}$)
ρ	Air density, proportion of static air pressure over the gas constant (R) multiplied by the air temperature (T)
ϕ	Phase lag between the W_f and E_v curves

DATA AVAILABILITY

Data will be made available upon reasonable request. Please see the link to Supplemental Material in "supplemental material."

SUPPLEMENTAL MATERIAL

Supplemental Figs. S1–S6 and Supplemental Table S1: https://doi.org/10.17605/OSF.IO/B5V8C.

ACKNOWLEDGMENTS

The authors thank the athletes for their enthusiastic participation in the study and Luca Ronchi, Donato Grassi, and Luca Riccobene for technical assistance at GVPM. Furthermore, we thank M. Legramandi and M. Pecchiari for the photographic record of the experiments.

Present address of G. Catavitello: Business and Decision Life Science Medical Communication Service Center, Brussels, Belgium. All other authors' affiliations correspond to their current address.

GRANTS

This study was funded by the Fonds de la Recherche Scientifique of Belgium (FNRS-CDR J.0200.22) and by "Tariffario Laboratorio Analisi" Research Fund, University of Milan (code RV_TAR16AMINE_M).

DISCLAIMERS

The content is solely the authors' responsibility and does not necessarily represent the official views of the UCLouvain, Politecnico di Milano, or the University of Milan.

DISCLOSURES

No conflicts of interest, financial or otherwise, are declared by the authors.

AUTHOR CONTRIBUTIONS

R.M.M., P.A.W., G.C., G.G., F.L., A.E.M., G.P., and A.H.D. conceived and designed research; R.M.M., P.A.W., G.C., G.G., F.L., A.E.M., G.P., and A.H.D. performed experiments; R.M.M., P.A.W., V.N., and A.H.D. analyzed data; R.M.M., P.A.W., V.N., and A.H.D. interpreted results of experiments; R.M.M., P.A.W., and A.H.D. prepared figures; R.M.M., P.A.W., G.C., G.G., V.N., F.L., A.E.M., G.P., and A.H.D. drafted manuscript; R.M.M., P.A.W., G.C., G.G., V.N., F.L., A.E.M., G.P., and A.H.D. edited and revised manuscript; R.M.M., P.A.W., G.C., G.G., V.N., F.L., A.E.M., G.P., and A.H.D. approved final version of manuscript.

REFERENCES

1. **Tucker VA.** The energetic cost of moving about: walking and running are extremely inefficient forms of locomotion. Much greater efficiency is achieved by birds, fish—and bicyclists. *Am Sci* 63: 413–419, 1975.
2. **Cavagna GA**, **Thys H**, **Zamboni A.** The sources of external work in level walking and running. *J Physiol* 262: 639–657, 1976. doi:10.1113/jphysiol.1976.sp011613.
3. **Cavagna GA**, **Heglund NC**, **Taylor CR.** Mechanical work in terrestrial locomotion: two basic mechanisms for minimizing energy expenditure. *Am J Physiol Regul Integr Comp Physiol* 233: R243–R261, 1977. doi:10.1152/ajpregu.1977.233.5.R243.
4. **Hoerner S.** *Fluid Dynamic Drag*. Hoboken, NJ: Wiley, 1965.
5. **Davies CT.** Effects of wind assistance and resistance on the forward motion of a runner. *J Appl Physiol Respir Environ Exerc Physiol* 48: 702–709, 1980. doi:10.1152/jappl.1980.48.4.702.
6. **Pecchiari MM**, **Legramandi MA**, **Gibertini G**, **Cavagna GA.** Still air resistance during walking and running. *Proc Biol Sci* 290: 20231763, 2023. doi:10.1098/rspb.2023.1763.
7. **Pugh LG.** Oxygen intake in track and treadmill running with observations on the effect of air resistance. *J Physiol* 207: 823–835, 1970. doi:10.1113/jphysiol.1970.sp009097.
8. **Pugh LG.** The influence of wind resistance in running and walking and the mechanical efficiency of work against horizontal or vertical forces. *J Physiol* 213: 255–276, 1971. doi:10.1113/jphysiol.1971.sp009381.
9. **Schickhofer L**, **Hanson H.** Aerodynamic effects and performance improvements of running in drafting formations. *J Biomech* 122: 110457, 2021.doi:10.1016/j.jbiomech.2021.110457.
10. **di Prampero P.** The energy cost of human locomotion on land and in water. *Int J Sports Med* 7: 55–72, 1986. doi:10.1055/s-2008-1025736.
11. **Hill AV.** The air-resistance to a runner. *Proc R Soc Lond B* 102: 380–385, 1928. doi:10.1098/rspb.1928.0012.
12. **Forte P**, **Sousa N**, **Teixeira J**, **Marinho D**, **Monteiro A**, **Bragada J**, **Morais J**, **Barbosa T.** Aerodynamic analysis of human walking, running and sprinting by numerical simulations. *Acta Bioeng Biomech* 24: 3–11, 2022. doi:10.37190/ABB-02019-2022-06. .
13. **Polidori G**, **Legrand F**, **Bogard F**, **Madaci F**, **Beaumont F.** Numerical investigation of the impact of Kenenisa Bekele's cooperative drafting strategy on its running power during the 2019 Berlin marathon. *J Biomech* 107: 109854, 2020. doi:10.1016/j.jbiomech.2020.109854.
14. **Marro M**, **Leckert J**, **Rollier E**, **Salizzoni P**, **Bailly C.** Wind tunnel evaluation of novel drafting formations for an elite marathon runner. *Proc R Soc A* 479: 20220836, 2023.doi:10.1098/rspa.2022.0836.
15. **Inoue T**, **Takafumi O**, **Takahiro T**, **Satoshi M**, **Katsuya H.** Wind-tunnel experiment on aerodynamic characteristics of a runner using a moving-belt system. *Cogent Eng* 3: 1231389, 2016. doi:10.1080/23311916.2016.1231389.
16. **Fernandes G**, **Gandur NL**, **Santos D**, **Maldonado V.** The sub 2-hour official marathon is possible: developing a drafting strategy for a historic breakthrough in sports (Preprint). Research Square, 2023. https://www.researchsquare.com/article/rs-3390553/v1 [accessed 2023 Dec 23].
17. **Mesquita RM**, **Dewolf AH**, **Catavitello G**, **Osgnach C**, **di Prampero PE**, **Willems PA.** The bouncing mechanism of running against hindering, or with aiding traction forces: a comparison with running on a slope. *Eur J Appl Physiol* 120: 1575–1589, 2020. doi:10.1007/s00421-020-04379-5.
18. **Da Silva ES**, **Kram R**, **Hoogkamer W.** The metabolic cost of emulated aerodynamic drag forces in marathon running. *J Appl Physiol (1985)* 133: 766–776, 2022. doi:10.1152/japplphysiol.00086.2022.
19. **Lloyd BB**, **Zacks RM.** The mechanical efficiency of treadmill running against a horizontal impeding force. *J Physiol* 223: 355–363, 1972. doi:10.1113/jphysiol.1972.sp009851.
20. **Chang YH**, **Kram R.** Metabolic cost of generating horizontal forces during human running. *J Appl Physiol (1985)* 86: 1657–1662, 1999. doi:10.1152/jappl.1999.86.5.1657.
21. **Valsecchi V**, **Gibertini G**, **Morelli A.** Wind tunnel test of drafting at endurance run velocity. *MMEP* 9: 27–35, 2022. doi:10.18280/mmep.090104.
22. **Beaumont F**, **Legrand F**, **Bogard F**, **Murer S**, **Vernede V**, **Polidori G.** Aerodynamic interaction between in-line runners: new insights on the drafting strategy in running. *Sports Biomech* : 1–16, 2021. Dec 7 doi:10.1080/14763141.2021.2006295.
23. **World Athletics.** World Record Progression of Marathon (Internet). 2023. https://worldathletics.org/records/by-progression/17427 [2024 Aug 21].
24. **Vogel S.** *Life in Moving Fluids: the Physical Biology of Flow* (2nd ed.). Princeton, NJ: Princeton University Press; 1994.
25. **Cavagna GA.** Symmetry and asymmetry in bouncing gaits. *Symmetry* 2: 1270–1321, 2010. Jun 25 doi:10.3390/sym2031270.
26. **Dewolf AH**, **Ivanenko YP**, **Mesquita RM**, **Lacquaniti F**, **Willems PA.** Neuromechanical adjustments when walking with an aiding or hindering horizontal force. *Eur J Appl Physiol* 120: 91–106, 2020. Jan doi:10.1007/s00421-019-04251-1.
27. **Dewolf AH**, **Peñailillo LE**, **Willems PA.** The rebound of the body during uphill and downhill running at different speeds. *J Exp Biol* 219: 2276–2288, 2016. doi:10.1242/jeb.142976.
28. **Dewolf AH**, **Ivanenko YP**, **Lacquaniti F**, **Willems PA.** Pendular energy transduction within the step during human walking on slopes at different speeds. *PLoS One* 12: e0186963–25, 2017. doi:10.1371/journal.pone.0186963.
29. **Minetti AE**, **Ardigò LP**, **Saibene F.** Mechanical determinants of gradient walking energetics in man. *J Physiol* 472: 725–735, 1993. doi:10.1113/jphysiol.1993.sp019969.
30. **Minetti AE**, **Ardigò LP**, **Saibene F.** Mechanical determinants of the minimum energy cost of gradient running in humans. *J Exp Biol* 195: 211–225, 1994. doi:10.1242/jeb.195.1.211.
31. **Cavagna GA**, **Willems PA**, **Legramandi MA**, **Heglund NC.** Within-step energy transduction. *J Exp Biol* 205: 3413–3422, 2002. doi:10.1242/jeb.205.21.3413.
32. **Dierick F**, **Penta M**, **Renaut D**, **Detrembleur C.** A force measuring treadmill in clinical gait analysis. *Gait Posture* 20: 299–303, 2004. doi:10.1016/j.gaitpost.2003.11.001.
33. **Winter DA.** *Biomechanics and Motor Control of Human Movement* (4th ed.). Hoboken, NJ: Wiley, 2009.

34. **Mesquita RM**, **Willems PA**, **Catavitello G**, **Dewolf AH.** Kinematics and mechanical changes with step frequency at different running speeds. *Eur J Appl Physiol* 124: 607–622, 2023. doi:10.1007/s00421-023-05303-3.
35. **Faul F**, **Erdfelder E**, **Lang AG**, **Buchner A.** G*Power 3: A flexible statistical power analysis program for the social, behavioral, and biomedical sciences. *Behav Res Methods* 39: 175–191, 2007. doi:10.3758/bf03193146.
36. **Mesquita RM**, **Willems PA**, **Dewolf AH**, **Catavitello G.** Kinetics and mechanical work done to move the body centre of mass along a curve. *PLoS One*19: e0298790, 2024. doi:10.1371/journal.pone.0298790.
37. **Gosseye TP**, **Willems PA**, **Heglund NC.** Biomechanical analysis of running in weightlessness on a treadmill equipped with a subject loading system. *Eur J Appl Physiol* 110: 709–728, 2010. doi:10.1007/s00421-010-1549-9.
38. **Cavagna GA**, **Saibene FP**, **Margaria R.** External work in walking. *J Appl Physiol* 18: 1–9, 1963. doi:10.1152/jappl.1963.18.1.1.
39. **Cavagna GA.** Force platforms as ergometers. *J Appl Physiol* 39: 174–179, 1975. doi:10.1152/jappl.1975.39.1.174.
40. **Willems PA**, **Cavagna GA**, **Heglund NC.** External, internal and total work in human locomotion. *J Exp Biol* 198: 379–393, 1995. doi:10.1242/jeb.198.2.379.
41. **Crouch TN**, **Burton D**, **Thompson MC**, **Brown NAT**, **Sheridan J.** Dynamic leg-motion and its effect on the aerodynamic performance of cyclists. *J Fluids Struct* 65: 121–137, 2016. doi:10.1016/j.jfluidstructs.2016.05.007.
42. **Nagahara R**, **Matsubayashi T**, **Matsuo A**, **Zushi K.** Kinematics of the thorax and pelvis during accelerated sprinting. *J Sports Med Phys Fitness* 58: 1253–1263, 2018. doi:10.23736/S0022-4707.17.07137-7.
43. **Cavagna GA**, **Willems PA**, **Franzetti P**, **Detrembleur C.** The two power limits conditioning step frequency in human running. *J Physiol* 437: 95–108, 1991. doi:10.1113/jphysiol.1991.sp018586.
44. **Novacheck TF.** The biomechanics of running. *Gait Posture* 7: 77–95, 1998. doi:10.1016/s0966-6362(97)00038-6.
45. **Warrener A**, **Tamai R**, **Lieberman DE.** The effect of trunk flexion angle on lower limb mechanics during running. *Hum Mov Sci* 78: 102817, 2021. doi:10.1016/j.humov.2021.102817.
46. **Folland JP**, **Allen SJ**, **Black MI**, **Handsaker JC**, **Forrester SE.** Running technique is an important component of running economy and performance. *Med Sci Sports Exerc* 49: 1412–1423, 2017. doi:10.1249/MSS.0000000000001245.
47. **van Oeveren BT**, **de Ruiter CJ**, **Beek PJ**, **van Dieën JH.** The biomechanics of running and running styles: a synthesis. *Sports Biomech* 23: 516–554, 2021. doi:10.1080/14763141.2021.1873411.
48. **Bramah C**, **Preece SJ**, **Gill N**, **Herrington L.** Is there a pathological gait associated with common soft tissue running injuries? *Am J Sports Med* 46: 3023–3031, 2018. doi:10.1177/0363546518793657.
49. **Mendiguchia J**, **Gonzalez De La Flor A**, **Mendez-Villanueva A**, **Morin JB**, **Edouard P**, **Garrues MA.** Training-induced changes in anterior pelvic tilt: potential implications for hamstring strain injuries management. *J Sports Sci* 39: 760–767, 2021. doi:10.1080/02640414.2020.1845439.
50. **Hoogkamer W**, **Kipp S**, **Frank JH**, **Farina EM**, **Luo G**, **Kram R.** A comparison of the energetic cost of running in marathon racing shoes. *Sports Med* 48: 1009–1019, 2018. doi:10.1007/s40279-017-0811-2.
51. **Hoogkamer W**, **Kram R**, **Arellano CJ.** How biomechanical improvements in running economy could break the 2-hour marathon barrier. *Sports Med* 47: 1739–1750, 2017. doi:10.1007/s40279-017-0708-0.
52. **Kyle CR**, **Caiozzo VJ.** The effect of athletic clothing aerodynamics upon running speed. *Med Sci Sports Exerc* 18: 509–515, 1986.
53. **Zamparo P**, **Pavei G**, **Nardello F**, **Bartolini D**, **Monte A**, **Minetti AE.** Mechanical work and efficiency of 5 + 5 m shuttle running. *Eur J Appl Physiol* 116: 1911–1919, 2016. doi:10.1007/s00421-016-3443-6.
54. **Peyré-Tartaruga LA**, **Coertjens M.** Locomotion as a powerful model to study integrative physiology: efficiency, economy, and power relationship. *Front Physiol* 9: 1789, 2018. doi:10.3389/fphys.2018.01789.
55. **Monte A**, **Nardello F**, **Magris R**, **Tecchio P**, **Zamparo P.** The influence of in vivo mechanical behaviour of the Achilles tendon on the mechanics, energetics and apparent efficiency of bouncing gaits. *J Exp Biol* 224: jeb242453, 2021. doi:10.1242/jeb.242453.
56. **Monte A**, **Maganaris C**, **Baltzopoulos V**, **Zamparo P.** The influence of Achilles tendon mechanical behaviour on “apparent” efficiency during running at different speeds. *Eur J Appl Physiol* 120: 2495–2505, 2020. doi:10.1007/s00421-020-04472-9.
57. **Farris DJ**, **Sawicki GS.** Human medial gastrocnemius force–velocity behavior shifts with locomotion speed and gait. *Proc Natl Acad Sci U S A* 109: 977–982, 2012. doi:10.1073/pnas.1107972109.
58. **Anderson BD.** The physics of sailing. *Physics Today* 61: 38–43, 2008. doi:10.1063/1.2883908.
59. **Jones AM**, **Doust JH.** A 1% treadmill grade most accurately reflects the energetic cost of outdoor running. *J Sports Sci* 14: 321–327, 1996. Aug doi:10.1080/02640419608727717.
60. **Miller JR**, **Van Hooren B**, **Bishop C**, **Buckley JD**, **Willy RW**, **Fuller JT.** A systematic review and meta-analysis of crossover studies comparing physiological, perceptual and performance measures between treadmill and overground running. *Sports Med* 49: 763–782, 2019. doi:10.1007/s40279-019-01087-9.
61. **Van Hooren B**, **Fuller JT**, **Buckley JD**, **Miller JR**, **Sewell K**, **Rao G**, **Barton C**, **Bishop C**, **Willy RW.** Is motorized treadmill running biomechanically comparable to overground running? A systematic review and meta-analysis of cross-over studies. *Sports Med* 50: 785–813, 2020. doi:10.1007/s40279-019-01237-z.
62. **di Prampero PE**, **Fusi S**, **Sepulcri L**, **Morin JB**, **Belli A**, **Antonutto G.** Sprint running: a new energetic approach. *J Exp Biol* 208: 2809–2816, 2005. doi:10.1242/jeb.01700.
63. **Mesquita RM**, **Dewolf AD.** Evaluation of mechanical workload using a GPS-tracking device. *Comp Method Biomech Biomed Eng* 25: S207, 2022.
64. **World Athletics.** *Competition Rules: Book C*. Port Hercules, Monaco: World Athletics, 2024.
65. **Taylor MJ**, **Beneke R.** Spring mass characteristics of the fastest men on Earth. *Int J Sports Med* 33: 667–670, 2012. doi:10.1055/s-0032-1306283.
66. **di Prampero PE**, **Osgnach C**, **Morin JB**, **Zamparo P**, **Pavei G.** Mechanical and metabolic power in accelerated running–part I: the 100-m dash. *Eur J Appl Physiol* 123: 2473–2481, 2023. doi:10.1007/s00421-023-05236-x.
67. **Donelan JM**, **Kram R**, **Kuo AD.** Mechanical work for step-to-step transitions is a major determinant of the metabolic cost of human walking. *J Exp Biol* 205: 3717–3727, 2002. doi:10.1242/jeb.205.23.3717.